Sugar-Based Polymers with Stereochemistry-Dependent Degradability and Mechanical Properties

Connor J. Stubbs,[#] Joshua C. Worch,[#] Hannah Prydderch, Zilu Wang, Robert T. Mathers, Andrey V. Dobrynin, Matthew L. Becker,* and Andrew P. Dove*

Read Online

ACCESS | Metrics & More | Article Recommendations | Supporting Information

ABSTRACT: Stereochemistry in polymers can be used as an effective tool to control the mechanical and physical properties of the resulting materials. Typically, though, in synthetic polymers, differences among polymer stereoisomers leads to incremental property variation, i.e., no changes to the baseline plastic or elastic behavior. Here we show that stereochemical differences in sugar-based monomers yield a family of nonsegmented, alternating polyurethanes that can be either strong amorphous thermoplastic elastomers with properties that exceed most cross-linked rubbers or robust, semicrystalline thermoplastics with properties comparable to commercial plastics. The stereochemical differences in the monomers direct distinct intra- and interchain supramolecular hydrogen-bonding interactions in the bulk materials to define their behavior. The chemical similarity among these isohexide-based polymers enables both statistical copolymerization and blending, which each afford independent control over degradability and mechanical properties. The modular molecular design of the polymers provides an opportunity to create a family of materials with divergent properties that possess inherently built degradability and outstanding mechanical performance.
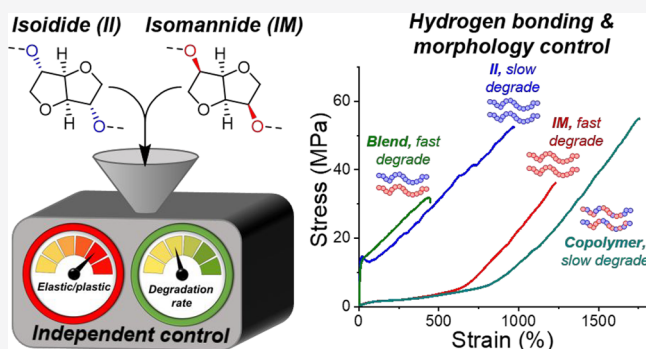
INTRODUCTION

The stereochemistry within synthetic polymer backbones is known to be critical to the performance of the resultant bulk polymeric materials. Polypropylene (PP), for example, possesses a methyl group at each repeat unit, and the stereochemical relationship of neighboring substituents (tacticity) significantly impacts chain-packing behavior. By increasing the stereoregularity of these neighboring units along the backbone (such as for isotactic polypropylene), polymer chains can pack more efficiently, increasing material crystallinity, which in turn results in dramatic improvements of the materials' strength and toughness.[1] Leading bioplastics, such as polylactic acid (PLA), have also begun utilizing stereochemistry to enhance thermomechanical properties.[2−4] However, unlike the fundamental difference in mechanical behavior observed in natural rubber (*cis*-1,4-polyisoprene), which is elastic, and gutta percha (*trans*-1,4-polyisoprene), which is plastic, both polypropylene and PLA retain plastic deformation under load irrespective of their stereochemistry or tacticity.

The unique structure and stereoisomerism found in natural compounds provide researchers with a strategic advantage in their endeavor toward creating mechanically robust materials in which stereochemistry can define the behavior.[5,6] Rigid-ring bicyclic ethers obtained from the dehydrative cyclization of su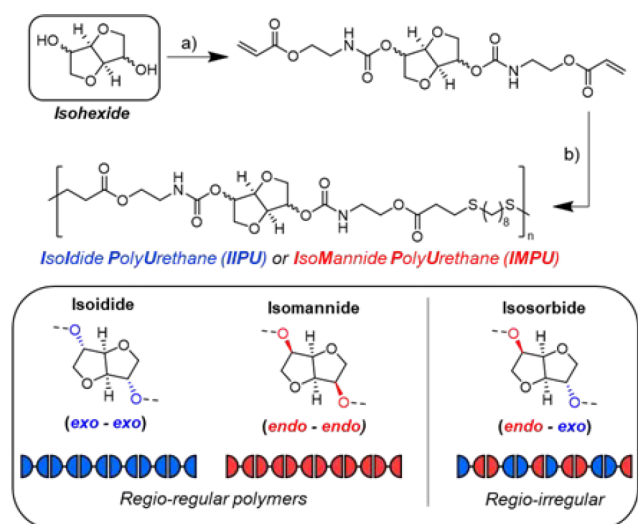gar hexitols have garnered substantial attention as monomers because of their unique structural features, imparting geometric isomerism (Scheme 1).[7−22] While the most prevalent of the biosourced cyclic units is the glucose-derived isosorbide, which is exemplified by its ubiquitous presence throughout polymer chemistry,[7,15] the accompanying stereoisomers, isomannide and isoidide, have received less attention. Some historic and recent studies have reported the synthesis of isomannide- and isoidide-containing polymers, but most lack detailed thermal and/or mechanical characterization to fully elucidate the influence of the stereochemistry. The isohexides all possess a bowl-shaped structure that results from the two fused tetrahydrofuranyl rings with the hydroxyl ring substituents in differing conformations. Beyond a few exceptions using ring-opening polymerization[23] or by polymerizing unsymmetrical isosorbide-based A−B monomers,[24] polymerization of isosorbide-based monomers leads to regioirregular polymers. We hypothesized, however, that the *endo−endo* conformation in isomannide and the *exo−exo* conformation in isoidide would
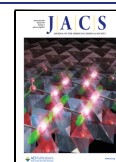
Scheme 1. Preparation of Isohexide-Containing Polyurethanes from Step-Growth Polymerization[a]

[a](a) 2-Isocyanatoethyl acrylate (2.4 equiv), dibutyltin dilaurate (5 mol %) in THF at 22 °C, 16 h; (b) 1,8-octanedithiol (1 equiv), dimethylphenylphosphine (1 mol %) in CHCl₃, −10 to 22 °C, 3 h.

provide an opportunity to investigate if the geometric isomerism of the isohexide could be leveraged to control the bulk thermomechanical properties of the materials, eliminating the effects of regiochemistry that are associated with the isosorbide derivative.

Herein, we report the synthesis and characterization of isoidide- and isomannide-based linear polymers (IIPU and IMPU, respectively) by embracing a chemical design that allows the influence of the isohexide stereochemistry on the properties of the resulting polymers to be probed. In contrast to synthetic polymers such as polypropylene and polylactide, but analogous to the unique behavior of the naturally derived natural rubber and gutta percha,[25] an unexpectedly sharp contrast in mechanical properties was observed between the plastic behavior of IIPU and the elastomeric behavior of IMPU. Computational investigations suggested the stereochemistry of the isohexide unit defines the supramolecular hydrogen-bonding interactions within the material, which in

turn define the mechanical properties. We further exploit these differences by copolymerizing stereoisomers and physically blending stereoisomeric homopolymers to tune hydrolytic degradability and thermomechanical properties independently of one another.

■ RESULTS AND DISCUSSION

Incorporation of the isoidide and isomannide stereoisomers into high molar mass polymers was achieved by step-growth polymerization of an isohexide-containing diacrylate (Figures S8−S11) with 1,8-octanedithiol using previously reported phosphine-catalyzed thiol-Michael polyaddition chemistry (Scheme 1).[26] While isomannide is a commercially available derivative, isoidide was synthesized through inversion of the isomannide stereochemistry using a facile protection and deprotection technique (Figure S1).[27] This overall approach is also analogous to recent protocols that employ a Mitsunobu reaction to invert the stereochemistry of isomannide.[28,29] The resultant alternating non-cross-linked homopolymers of IIPU and IMPU were well-defined, nonsegmented, regioregular polymers (Figures S12−S15). The polymers were isolated by direct precipitation from the reaction mixture at a high molecular weight with broad molar mass distribution, $Đ_M$ (IIPU − M_w = 117 kDa, $Đ_M$ = 8.12; IMPU − M_w = 95 kDa, $Đ_M$ = 9.69), which was expected as a result of irreversible formation of cyclic oligomers in the step-growth polymerization (Figure S25).[30] The non-cross-linked architecture is supported by analysis of the materials using size-exclusion chromatography coupled with viscometry detection (Figure S26). The results revealed α values ranging from 0.51 to 0.58, which is indicative of a linear, unbranched, or non-cross-linked material in a theta/good solvent.[31]

Key to our monomer design was the internal urethane units, which we reasoned would enhance thermomechanical properties by promoting a strong hydrogen-bonding network[32] and complementing the rigidity of the bicyclic isohexide geometry. IIPU and IMPU both possess high thermal stabilities that enabled facile processing (heated compression molding) into a flexible, free-standing film suitable for mechanical analysis (Figure S28). We observed that thermally processed IIPU became less transparent (indicative of crystallization) within hours of processing, so both IIPU and IMPU films were
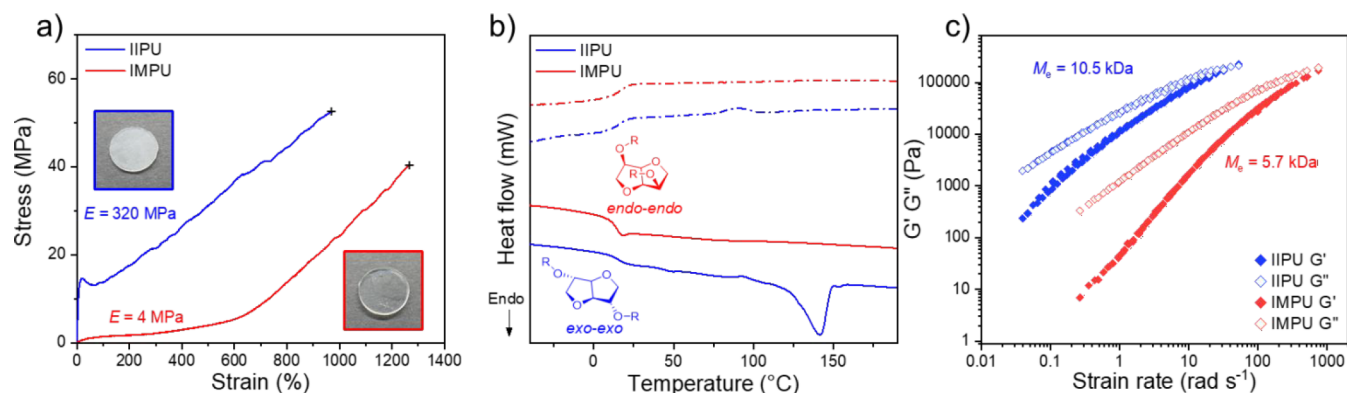

Figure 1. Thermomechanical analysis of IIPU and IMPU. (a) Representative stress vs strain curves obtained at 10 mm·min⁻¹, 22 °C for annealed IIPU and IMPU with Young's modulus (E) displayed (inset: photographs of pressed films of IIPU and IMPU). (b) DSC thermograms of the first heating and cooling cycle for the annealed (3 days, 22 °C) IIPU and IMPU (solid line = heating scan and dashed line = cooling scan). (c) Time−temperature superposition of rheological frequency sweeps of IIPU and IMPU overlaid at 130 °C. Chain entanglement molecular weight (M_e) of IIPU and IMPU is displayed.

annealed for 3 days at ambient temperature (22 °C) before testing to ensure a thermal equilibrium had been reached (see Supporting Information for details). The mechanical properties of the annealed isohexide polymers were assessed using uniaxial tensile testing until failure (Figure 1a, Figure S29). Both IIPU and IMPU possessed a significant strain hardening feature leading to high ultimate tensile strength (UTS) and tensile toughness (Table S3). IIPU exhibited a moderate Young's modulus (320 ± 66 MPa) and a distinct yield point as the material entered the plastic deformation region, the latter of which is a feature common to thermoplastic materials. The stiffness and ductility of IIPU were comparable to commodity polyolefins, such as high-density polyethylene (HDPE) (Figure S30). However, the strain hardening phenomenon exhibited in IIPU (onset near ∼100% strain) resulted in a high UTS that was more comparable to Nylon-6 (Table S3). The tough plastic behavior of IIPU was starkly contrasted against the softer elastomeric nature of IMPU, illustrated by their nearly 2 order of magnitude difference in the Young's moduli (IIPU E = 320 MPa, IMPU E = 4 MPa) (Figure 1a, Figure S29, Table S3). In addition, IMPU displayed excellent recovery after deformation (Figure S31), which corroborates the absence of a yield point in the tensile analysis. To investigate the possibility that the robust mechanical properties of both IIPU and IMPU were influenced by their large molar mass distributions ($Đ_M$ > 8), both polymers were prepared with a lower dispersity ($Đ_M$ < 3) and assessed using tensile analysis. Consistent general tensile behavior was observed between each respective polymer; that is, IMPU was a strong elastomer and IIPU was a tough plastic regardless of dispersity values (Figure S32, Table S3). The IMPU samples were nearly indistinguishable in their mechanical metrics. However, for IIPU, the tensile strength and strain at break were decreased somewhat in the sample with lower dispersity, but this can be explained by the comparatively lower molar mass of that polymer (M_w = 37 kDa).

Typically, creating materials with mechanical properties that are as divergent as IIPU and IMPU requires significant microstructure changes to the polymer architecture (such as altering composition, topology, and/or cross-linking); that is, one must "redesign" the polymer system. Here, the profound difference in thermomechanical properties appears to be solely attributed to the stereochemical differences between the isohexide moieties. The significance of the isohexide moiety to the polymer architecture and ultimate performance can be further evidenced by comparison to an analogous study of alkene-containing polyurethanes.[26] In that study, the *cis/trans* stereoisomerism indeed influenced the mechanical properties of the materials, but the effect was modest and all unsaturated polymers displayed plastic-like behavior irrespective of the stereoisomer. This behavior has also been observed in polymers that contain double bonds, synthesized by nucleophilic thiol-yne addition, in which the materials retain a yield point and hence display plastic deformation, even despite significant differences in mechanical behavior.[33−36] To our knowledge, the only exceptions from this behavior are natural rubber and gutta percha (poly(*cis*-isoprene) and poly(*trans*-isoprene), respectively) and a recent report of a cross-linked photoset material in which constraints imposed by the network formation prevent association of the oligomeric chains when low molar mass oligomers are used.[37]

Encouraged by the divergent mechanical behavior of the isomeric polymers, we then examined the influence of

stereochemistry on the thermal properties. Annealed thin films of IIPU and IMPU were compared using differential scanning calorimetry (Figure 1b, Figure S33). Both IIPU and IMPU were found to possess single glass transitions around the same temperature (T_g ≈ 15 °C), which suggests that the alternating structure of the polymer prevents bulk phase separation. However, the DSC thermograms indicated a distinct difference between the materials at higher temperatures. The prominent endothermic peak (from 111 to 158 °C) observed in the first IIPU heating cycle is characteristic of a first-order phase transition (T_m). Subsequent heating cycles display an exothermic cold crystallization peak (T_{cc}) before again melting, due to an inability to crystallize in the cooling cycle time frame. These features are notably absent for the IMPU sample, which indicates that the IIPU is semicrystalline, while the IMPU sample appears to be amorphous. Annealing IIPU at a higher temperature resulted in no significant changes to the crystallinity or overall thermal profile of the polymer (Figure S34).

To further understand how the isohexide structure influenced the polymer chain interactions, rheological frequency sweeps were performed on IIPU and IMPU at various temperatures (Figure 1c). From this measurement, the molecular weight between polymer entanglements (M_e) can be calculated from fitting the rheology data with a reptation model (Figure S38).[38] IIPU was calculated to have a larger M_e (M_e = 10.5 kDa, G_e = 1.8 MPa) than IMPU (M_e = 5.7 kDa, G_e = 5.3 MPa), which indicates that the isoidide stereochemistry leads to polymer chains that are more linear, or less entangled, in comparison to isomannide.

We performed detailed molecular dynamics simulations to highlight the origin of the opposing mechanical properties of the IIPU and IMPU polymers (Figures S39 and S40). Evolution of the macromolecular conformations of two intertwined IIPU macromolecules upon deformation (snapshots shown in Figure 2a) revealed that the IIPU macromolecules have a large number of both inter- and intramolecular H-bonds in the undeformed state (Figure 2b). In fact, an almost equal number of intra- and intermolecular H-bonds is indicated by the observed ratio close to unity. A similar analysis of the effect of the macromolecular elongation on intermolecular interactions demonstrates striking differences between structural transformations in IIPU and IMPU (Figure 2b). Under increasing deformation, the number of intramolecular H-bonds decreases for both systems, while the number of intermolecular bonds remains constant for IIPU yet increases for IMPU. We postulated that this preference for formation of the intermolecular associations in IIPU chains could be the reason that this polymer crystallizes. To further understand the origin of crystallinity in the IIPU polymer materials, we performed molecular dynamics simulations of the bulk systems consisting of 75 IIPU repeat units with a degree of polymerization, DP, of 16, at a polymer density of 0.95 g·cm⁻³, temperature T = 300 K, and pressure P = 1.0 atm and compared them to an equivalent system with IMPU chains (Figure S40). These simulations show that IIPU forms approximately 50% more H-bonds than IMPU and is a direct consequence of the differences in the local molecular conformations (Figure S40). Furthermore, unlike IMPU, IIPU is capable of forming strong H-bonded associations, which could be viewed as precursors of IIPU chain crystallization. The observed divergence in properties between isoidide- and isomannide-based materials highlights the power
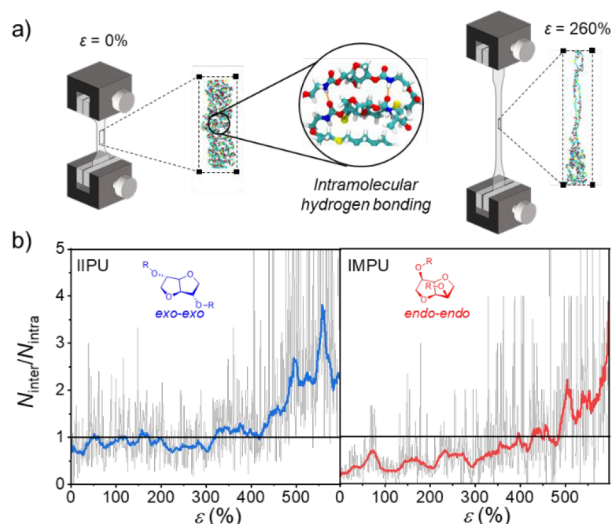
Figure 2. Molecular dynamic simulations of hydrogen bonding in IIPU and IMPU under deformation. (a) Snapshots illustrating the conformational changes of IIPU macromolecules under deformation and highlighting the observed intramolecular hydrogen bonding. (b) Dependence of the ratio of the intermolecular (N_{inter}) hydrogen bonds to intramolecular (N_{intra}) hydrogen bonds on deformation for IIPU (left) and IMPU (right) systems. Data were averaged over 20 different simulation runs from undeformed state.

of controlling supramolecular interactions via stereochemistry (especially ring-induced geometric isomerism) in renewable monomer feedstocks. This is in line with a recent study of chemically analogous, carbohydrate-derived isosorbide- and glucarodilactone-based thermosets that demonstrated significant mechanical differences as a consequence of divergent chain interactions; however the samples both displayed elastomeric behavior.[39]

The disparity of mechanical properties juxtaposed against the chemical similarity between IIPU and IMPU presented the opportunity to finely manipulate material mechanical properties by combining the stereoisomers either in physical blends or by copolymerization. Statistical copolymers (co-II$_x$IM$_y$) with controlled stereochemical composition were obtained by varying the relative quantity of isoidide and isomannide monomer in the feed and copolymerizing with 1,8-octanedithiol to afford polymers. ^{1}H NMR spectroscopy confirmed the feed ratios of isomannide and isoidide were retained in the final polymer (Figure S41). The copolymer with 75% isoidide content (co-II$_{75}$IM$_{25}$) was semicrystalline, albeit with a significant reduction in overall crystallinity as evidenced by a decrease of 9 J·g^{-1} in the total enthalpy of melting (ΔH_m) compared to IIPU (Figure S35a, Table S3). A significant decrease in the polymer melting range was also observed ($\Delta T_m \approx 60$ °C, Table S3). The semicrystalline co-II$_{75}$IM$_{25}$ behaved like a plastic, albeit with a reduction in overall material toughness and modulus as compared to IIPU (Figures S42a and S43). Below 75% isoidide content,
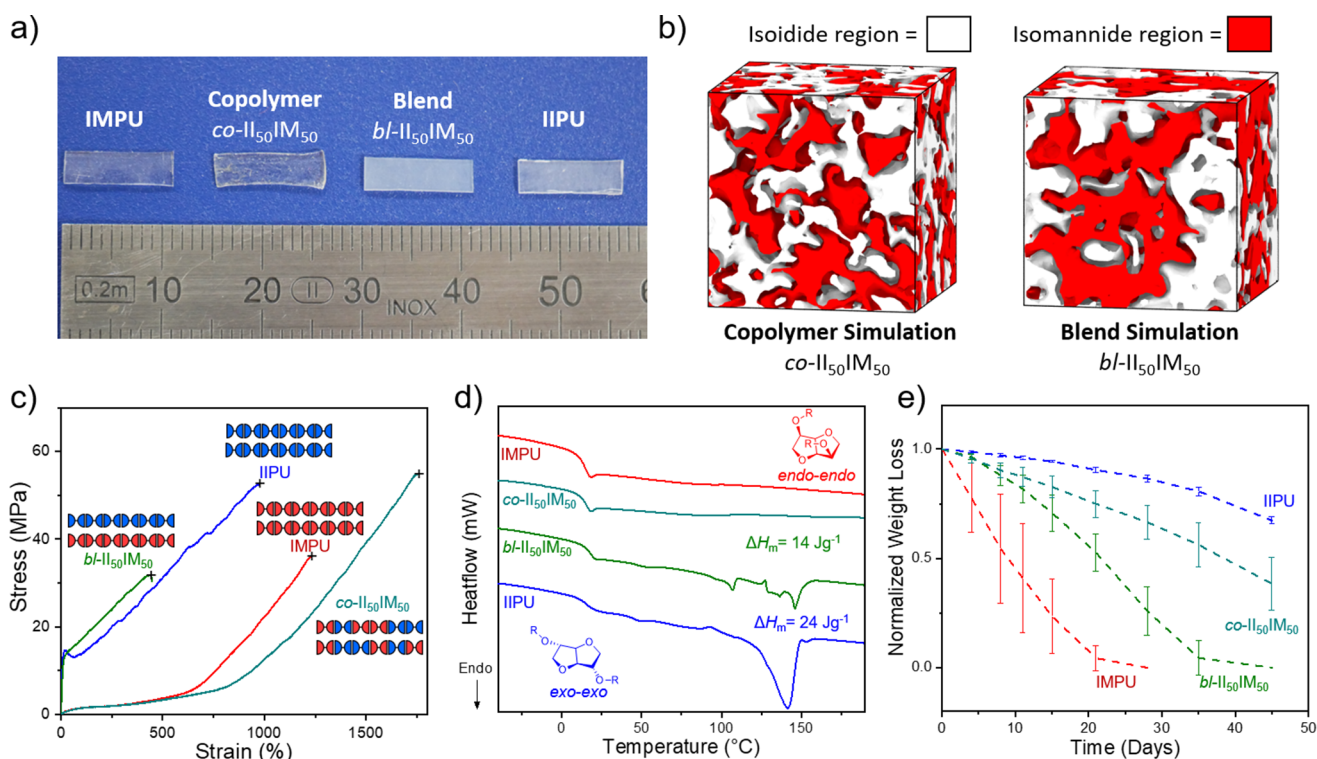

Figure 3. (a) Image of heat-compressed IIPU, IMPU, co-II$_{50}$IM$_{50}$, and bl-II$_{50}$IM$_{50}$ to illustrate crystallinity differences. (b) Bulk system simulations of co-II$_{50}$IM$_{50}$ and bl-II$_{50}$IM$_{50}$ illustrating the separation of isoidide (white) and isomannide (red) regions. (c) DSC thermograms of the first heating cycle of annealed IIPU, IMPU, co-II$_{50}$IM$_{50}$, and bl-II$_{50}$IM$_{50}$ at 10 K·min^{-1}. Total enthalpy of melting (ΔH_m) calculated from integration of all melting transitions. (d) Representative stress vs strain tensile curves of annealed IIPU, IMPU, and both statistical copolymers and a physical blend at 50/50 II/IM ($n > 3$). Mechanical testing was performed at 10 mm·min^{-1}. (e) Normalized weight loss of IIPU, IMPU, co-II$_{50}$IM$_{50}$, and bl-II$_{50}$IM$_{50}$ discs in 1 M NaOH$_{(aq)}$ over 45 days at 25 °C. $n = 3$. (f) Table summarizing thermomechanical properties of blend and copolymer in comparison to IIPU and IMPU homopolymers: [a]Young's modulus; [b]ultimate tensile strength (UTS); [c]strain at break.

copolymer thermal properties were more influenced by isomannide than isoidide and resulted in a series of amorphous thermoplastic elastomers (Figure S35b,c). Both co-II$_{50}$IM$_{50}$ and co-II$_{25}$IM$_{75}$ presented with a similar tensile profile (J-shaped curve) to the elastomeric IMPU sample and a statistically significant ($P < 0.05$) increase in both strength and toughness compared to IMPU (Figures S42b,c and S43, Table S3). Together these observations suggest that the presence of small amounts of isoidide enhanced the mechanical performance of co-II$_{50}$IM$_{50}$ and co-II$_{25}$IM$_{75}$ without imparting crystallinity to the samples, in contrast to the stereopure IIPU or 75% II formulations. This feature also adds to the capacity of isoidide as an attractive sustainable comonomer to improve toughness in existing thermoplastic elastomer designs.

Physical blending of polymers provides a rapid and convenient method to access a range of properties between two or more distinctly different polymers; however it can be practically challenging to achieve desirable physical properties in the resultant material. In many cases, immiscibility between polymers dominates, even where the structures are very similar (i.e., polypropylene and polyethylene), unless specific compatibilization efforts are applied. The inherent incompatibility often leads to macroscopic phase separation, or defects, in the blended sample, which contributes to poor mechanical performance.[40] Moreover, miscibility limitations can be even more exaggerated in binary blends derived from a semicrystalline/amorphous polymer mixture,[41] but could offer advantages in mechanical recycling of these materials. Despite IIPU and IMPU possessing distinctly different thermomechanical properties (IIPU, semicrystalline, plastic; IMPU, amorphous elastomer), blending of these two polymers was accomplished without any complex compatibilization requirements and yielded macroscopically homogeneous films (Figure 3a), presumably as a result of the isomeric nature of the polymers. Polymer blends with varying quantities of IMPU and IIPU (Figures S22−S24 and S27, Table S3) were made by a simple dissolution−precipitation method and then melt processed into uniform films after drying. In contrast to the copolymer samples, all physical blends were semicrystalline, but they exhibited more complex melting behaviors compared to IIPU (Figure 3d). Specifically, the physical blends exhibited multifeatured DSC profiles, possibly due to multiple crystalline domains within the samples, with melting ranges between that of the IIPU homopolymer (Figure S36, Table S3). Surprisingly, the ΔH_m for the blended films is greater than expected when normalized to the molar content of isoidide in the sample (Table S3). The presence of IMPU homopolymer appeared to enhance the crystallization efficiency of IIPU, which is a similar phenomenon previously reported in cis- or $trans$-rich polyisoprene blends.[42] The semicrystalline nature of the blended samples also imbued them with tough plastic behavior, analogous to IIPU (Figure 3c, Figures S44 and S45). Many polymerization methods prevent the copolymerization of monomers that produce materials with dramatically different mechanical properties, and, commonly, blending of polymers results in bulk phase separation to produce plastics that have inferior properties to their respective homopolymers.[43−49] Here, however, the postblending compatibility enabled materials with practical mechanical properties (Figure 3f). This offers further opportunity to retain the excellent material properties of IIPU and has potential application for mechanical recycling of mixed polymer feeds.

To understand the differences between copolymers and blends, we undertook molecular dynamics simulations of each bulk system. In both samples, there was a distinct regional separation between the isoidide and isomannide domains (Figure 3b). The copolymer simulations showed the formation of a greater number of smaller domains, which indicates that this microstructure facilitates better separation between II- and IM-rich regions than is possible in the physical blends. This was further quantified by calculating the interfacial surface area per unit volume between the II and IM domains (Figure 3b and Figure S47) with a lower surface area being calculated in each case for physical blends (i.e., bl-II$_{50}$IM$_{50}$ = 0.9297 Å^{-1}) in comparison to the copolymers (i.e., co-II$_{50}$IM$_{50}$ = 1.4399 Å^{-1}) at the same II/IM molar ratio. We postulate that the larger IIPU domains in the physical blends facilitate crystallization of the IIPU regions and hence promotes the plastic behavior. This was further investigated using AFM to study the surface morphology of co-II$_{50}$IM$_{50}$ and bl-II$_{50}$IM$_{50}$. Evidence for phase separation is shown within the physically blended sample, while the copolymer sample exhibits a more homogeneous morphology (Figures S47−48).

Petroleum-derived plastics are notorious for their environmental persistence, even under extreme conditions, due to the hydrophobicity and homogeneity imparted by their all carbon-based backbones.[50] Without useful chemical "trigger" points (such as oxygen and nitrogen) in the backbone of polymers,[51] environmental degradation processes are limited and slow, and hence we also sought to demonstrate that hydrolytic degradation could provide a further advantage for our sustainable thermoplastic materials over traditional petrochemical-derived plastics. A straightforward accelerated degradation experiment was used to study this process in a rapid manner. Thin discs (ca. 0.5 mm thickness) of IIPU and IMPU were placed in 1 M NaOH$_{(aq)}$, to assess the influence of stereochemistry and composition on the rate of hydrolytic degradation (Figure 3e). Polymer crystallinity is known to inhibit hydrolytic degradation by restricting water penetration into the bulk sample,[52] and hence we postulated that differences in degradation between IIPU and IMPU would be largely regulated by crystallinity. Although IIPU degraded at a slower rate than amorphous IMPU, the sample still exhibited significant mass loss within the time frame of the study (~25% mass loss within 45 days), showing its potential to degrade by hydrolysis, should it be released into the environment, or for chemical depolymerization methods[53,54] such as those used for the chemical recycling of PET.

Exploration of the hydrolytic degradation of the copolymers and physical blends revealed that the mechanical behavior (plastic vs elastic) could be decoupled from the inherent hydrolytic degradation. Studying the accelerated hydrolysis of the crystalline polymer blend (bl-II$_{50}$IM$_{50}$) and the analogous amorphous copolymer (co-II$_{50}$IM$_{50}$) under the same conditions revealed that bl-II$_{50}$IM$_{50}$ degraded far more rapidly than IIPU, even though the thermomechanical properties were comparable (Figure 3c−e). On the contrary, co-II$_{50}$IM$_{50}$ degraded significantly slower than the IMPU despite both materials being amorphous and possessing similar T_gs. The wettability of each homopolymer and corresponding 50:50 physical blend or copolymer formulation was investigated using the contact angle of the water−polymer interface (Figure S49). The semicrystalline bl-II$_{50}$IM$_{50}$ was observed to be less hydrophilic than the amorphous co-II$_{50}$IM$_{50}$, which suggests that this property is not driving its increased degradation rate

compared to the copolymer sample (Table S1). However, the contrasting degradation behaviors are consistent with the separation of II and IM domains within copolymers and physical blends (Figure 3b, Figure S48), such that the slower degradation of the copolymer is influenced by the II-based domains, which are smaller and more evenly dispersed throughout the bulk system; the greater separation of domains in the blended system leads to a degradation rate that is more influenced by the IMPU. Previous systems with degradability control based on microstructure have required precision-made sequences;[55−58] however the simplicity of the approach herein lends to the opportunity to tune mechanical properties independent of degradation.

Finally, to further explore the degradation behavior of IMPU and IIPU and understand how they might degrade in the ocean, a combination of experimental and calculated physical property data was used to predict quantitative and qualitative degradation profiles.[59] Using a qualitative model, classification trees converted physical property data to degradation categories (i.e., fast, medium, slow) and placed both IIPU and IMPU as "medium", alongside polymers that are well known to degrade in the environment (i.e., polyhydroxybutyrate). To calculate a quantitative degradation profile for biotic and abiotic conditions, we adopted an equation based on seawater temperature (T_{water}), T_g, crystallinity, and $\log P(SA)^{-1}$ (as a measure of hydrophobicity) to calculate relative rates (k_{rel}) of seawater degradation. IIPU and IMPU offer a unique balance of physical properties that should facilitate seawater degradation including T_g values < ocean temperature, low degrees of hydrophobicity [i.e., $\log P(SA)^{-1}$],[60−62] and minimal crystallinity. To quantify the contribution of abiotic hydrolysis to degradation, we screened physical property data, including relative rates for degradation experiments in NaOH(aq), and gained insight from a degradation database (which contains similar functional groups to those found in IIPU and IMPU)[59] to propose a simple model to predict k_{rel} values (Figures S50−51, and Table S2). As such, the predicted rate of degradation of IIPU in seawater is comparable to poly(ϵ-caprolactone), PCL, and is faster by approximately an order of magnitude when compared to PLA (Figure 4). Furthermore, IMPU is predicted to degrade approximately an order of magnitude faster than IIPU (i.e., 2 orders of magnitude faster than PLA).

CONCLUSION

The complex structure and stereoisomerism found in natural compounds provide a strategic advantage in the endeavor toward creating mechanically robust sustainable materials. The difference in fundamental deformation behavior between isosorbide- and isomannide-based materials, as well as their outstanding mechanical features in their own right, is testament to the potential of leveraging stereochemistry to direct supramolecular interactions in biosourced monomer feedstocks. However, the most outstanding feature of this system is the distinct property difference arising from stereochemically distinct hydrogen bonding in otherwise compositionally and stoichiometrically identical materials. Here, we have shown the ability to independently tune, or decouple, the hydrolytic degradation rate from the thermomechanical properties while also controlling these features through simple copolymerization or blending strategies. Simply put, the exhibition of intricate property manipulation presented herein is unparalleled in the state-of-the-art materials
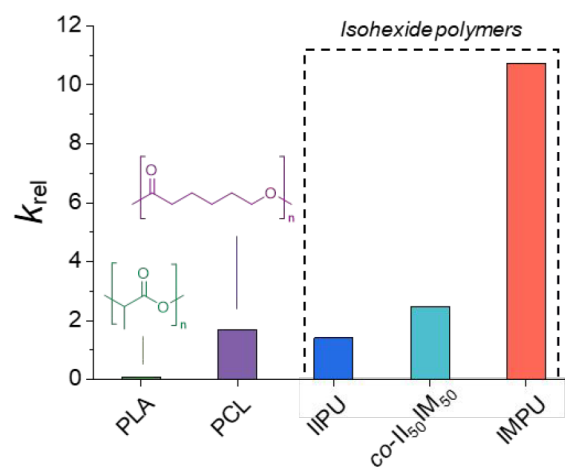

Figure 4. Calculated k_{rel} values for predicted seawater degradation of isohexide-based polymers and degradable commercial polymers: PLA and PCL.

portfolio and affords a path to materials with on-demand property tuning that is made possible only by stereochemistry manipulation.

ASSOCIATED CONTENT

Supporting Information

The Supporting Information is available free of charge at https://pubs.acs.org/doi/10.1021/jacs.1c10278.

All synthetic procedures, characterization, and thermomechanical analysis (PDF)

AUTHOR INFORMATION

Corresponding Authors

Matthew L. Becker − *Department of Chemistry, Mechanical Engineering and Materials Science, Biomedical Engineering and Orthopedic Surgery, Duke University, Durham, North Carolina 20899, United States;* orcid.org/0000-0003-4089-6916; Email: Matthew.L.Becker@duke.edu

Andrew P. Dove − *School of Chemistry, The University of Birmingham, Birmingham B15 2TT, U.K.;* orcid.org/0000-0001-8208-9309; Email: A.Dove@bham.ac.uk

Authors

Connor J. Stubbs − *School of Chemistry, The University of Birmingham, Birmingham B15 2TT, U.K.*

Joshua C. Worch − *School of Chemistry, The University of Birmingham, Birmingham B15 2TT, U.K.;* orcid.org/0000-0002-4354-8303

Hannah Prydderch − *School of Chemistry, The University of Birmingham, Birmingham B15 2TT, U.K.*

Zilu Wang − *Department of Chemistry, University of North Carolina−Chapel Hill, Chapel Hill, North Carolina 27599, United States;* orcid.org/0000-0002-5957-8064

Robert T. Mathers − *Department of Chemistry, Pennsylvania State University, New Kensington, Pennsylvania 15068, United States;* orcid.org/0000-0002-0503-4571

Andrey V. Dobrynin − *Department of Chemistry, University of North Carolina−Chapel Hill, Chapel Hill, North Carolina 27599, United States;* orcid.org/0000-0002-6484-7409

Complete contact information is available at:
https://pubs.acs.org/10.1021/jacs.1c10278

■ **REFERENCES**

(1) Natta, G.; Pino, P.; Corradini, P.; Danusso, F.; Mantica, E.; Mazzanti, G.; Moraglio, G. Crystalline high polymers of α-olefins. *J. Am. Chem. Soc.* **1955**, 77 (6), 1708−1710.
(2) Chile, L.-E.; Mehrkhodavandi, P.; Hatzikiriakos, S. G. A comparison of the rheological and mechanical properties of isotactic, syndiotactic, and heterotactic Poly(lactide). *Macromolecules* **2016**, 49 (3), 909−919.
(3) Farah, S.; Anderson, D. G.; Langer, R. Physical and mechanical properties of PLA, and their functions in widespread applications — A comprehensive review. *Adv. Drug Delivery Rev.* **2016**, 107, 367−392.
(4) Garlotta, D. A literature review of poly(lactic acid). *J. Polym. Environ.* **2001**, 9 (2), 63−84.
(5) Schneiderman, D. K.; Hillmyer, M. A. 50th Anniversary perspective: There is a great future in sustainable polymers. *Macromolecules* **2017**, 50 (10), 3733−3749.
(6) Zhu, Y.; Romain, C.; Williams, C. K. Sustainable polymers from renewable resources. *Nature* **2016**, 540 (7633), 354−362.
(7) Saxon, D. J.; Luke, A. M.; Sajjad, H.; Tolman, W. B.; Reineke, T. M. Next-generation polymers: Isosorbide as a renewable alternative. *Prog. Polym. Sci.* **2020**, 101, 101196.
(8) Qian, W.; Liu, L.; Zhang, Z.; Su, Q.; Zhao, W.; Cheng, W.; Dong, L.; Yang, Z.; Bai, R.; Xu, F.; Zhang, Y.; Zhang, S. Synthesis of bioderived polycarbonates with adjustable molecular weights catalyzed by phenolic-derived ionic liquids. *Green Chem.* **2020**, 22 (8), 2488−2497.
(9) Legrand, S.; Jacquel, N.; Amedro, H.; Saint-Loup, R.; Pascault, J.-P.; Rousseau, A.; Fenouillot, F. Synthesis and properties of poly(1,4-cyclohexanedimethylene-co-isosorbide terephthalate), a bio-based copolyester with high performances. *Eur. Polym. J.* **2019**, 115, 22−29.
(10) Hu, C.; Bourbigot, S.; Delaunay, T.; Collinet, M.; Marcille, S.; Fontaine, G. Synthesis of isosorbide based flame retardants: Application for polybutylene succinate. *Polym. Degrad. Stab.* **2019**, 164, 9−17.
(11) Park, S.-A.; Jeon, H.; Kim, H.; Shin, S.-H.; Choy, S.; Hwang, D. S.; Koo, J. M.; Jegal, J.; Hwang, S. Y.; Park, J.; Oh, D. X. Sustainable and recyclable super engineering thermoplastic from biorenewable monomer. *Nat. Commun.* **2019**, 10 (1), 2601.
(12) Park, S.-A.; Im, C.; Oh, D. X.; Hwang, S. Y.; Jegal, J.; Kim, J. H.; Chang, Y.-W.; Jeon, H.; Park, J. Study on the synthetic characteristics of biomass-derived isosorbide-based poly(arylene ether ketone)s for sustainable super engineering plastic. *Molecules* **2019**, 24 (13), 2492.
(13) Vijjamarri, S.; Hull, M.; Kolodka, E.; Du, G. Renewable isohexide-based, hydrolytically degradable poly(silyl ether)s with high thermal stability. *ChemSusChem* **2018**, 11 (17), 2881−2888.
(14) Ji, X.; Wang, Z.; Wang, Z.; Yan, J. Bio-based poly(ether imide)s from isohexide-derived isomeric dianhydrides. *Polymers* **2017**, 9 (11), 569.
(15) Galbis, J. A.; García-Martín, M. d. G.; de Paz, M. V.; Galbis, E. Synthetic polymers from sugar-based monomers. *Chem. Rev.* **2016**, 116 (3), 1600−1636.
(16) Gallagher, J. J.; Hillmyer, M. A.; Reineke, T. M. Acrylic triblock copolymers incorporating isosorbide for pressure sensitive adhesives. *ACS Sustainable Chem. Eng.* **2016**, 4 (6), 3379−3387.
(17) Wroblewska, A.; Zych, A.; Thiyagarajan, S.; Dudenko, D.; van Es, D.; Hansen, M. R.; Koning, C.; Duchateau, R.; Jasinska-Walc, L. Towards sugar-derived polyamides as environmentally friendly materials. *Polym. Chem.* **2015**, 6 (22), 4133−4143.
(18) Javni, I.; Bilić, O.; Bilić, N.; Petrović, Z. S.; Eastwood, E. A.; Zhang, F.; Ilavský, J. Thermoplastic polyurethanes with isosorbide chain extender. *J. Appl. Polym. Sci.* **2015**, 132 (47), 42830.
(19) Gallagher, J. J.; Hillmyer, M. A.; Reineke, T. M. Isosorbide-based polymethacrylates. *ACS Sustainable Chem. Eng.* **2015**, 3 (4), 662−667.
(20) Lavilla, C.; Muñoz-Guerra, S. Sugar-based aromatic copolyesters: A comparative study regarding isosorbide and diacetalized alditols as sustainable comonomers. *Green Chem.* **2013**, 15 (1), 144−151.
(21) Nelson, A. M.; Long, T. E. A perspective on emerging polymer technologies for bisphenol-A replacement. *Polym. Int.* **2012**, 61 (10), 1485−1491.
(22) Bachmann, F.; Reimer, J.; Ruppenstein, M.; Thiem, J. Synthesis of novel polyurethanes and polyureas by polyaddition reactions of dianhydrohexitol configured diisocyanates. *Macromol. Chem. Phys.* **2001**, 202 (17), 3410−3419.
(23) Saxon, D. J.; Nasiri, M.; Mandal, M.; Maduskar, S.; Dauenhauer, P. J.; Cramer, C. J.; LaPointe, A. M.; Reineke, T. M. Architectural control of isosorbide-based polyethers via ring-opening polymerization. *J. Am. Chem. Soc.* **2019**, 141 (13), 5107−5111.
(24) Besset, C.; Binauld, S.; Ibert, M.; Fuertes, P.; Pascault, J.-P.; Fleury, E.; Bernard, J.; Drockenmuller, E. Copper-catalyzed vs thermal step growth polymerization of starch-derived α-azide−ω-alkyne dianhydrohexitol stereoisomers: To click or not to click? *Macromolecules* **2010**, 43 (1), 17−19.
(25) Worch, J. C.; Prydderch, H.; Jimaja, S.; Bexis, P.; Becker, M. L.; Dove, A. P. Stereochemical enhancement of polymer properties. *Nat. Rev. Chem.* **2019**, 3 (9), 514−535.
(26) Stubbs, C. J.; Worch, J. C.; Prydderch, H.; Becker, M. L.; Dove, A. P. Unsaturated poly(ester-urethanes) with stereochemically dependent thermomechanical properties. *Macromolecules* **2020**, 53 (1), 174−181.
(27) Cope, A. C.; Shen, T. Y. The stereochemistry of 1,4:3,6-dianhydrohexitol derivatives. *J. Am. Chem. Soc.* **1956**, 78 (13), 3177−3182.
(28) Rajput, B. S.; Gaikwad, S. R.; Menon, S. K.; Chikkali, S. H. Sustainable polyacetals from isohexides. *Green Chem.* **2014**, 16 (8), 3810−3818.
(29) Gormong, E. A.; Reineke, T. M.; Hoye, T. R. Synthesis of isohexide diyne polymers and hydrogenation to their saturated polyethers. *ACS Macro Lett.* **2021**, 10 (8), 1068−1072.
(30) Yong Choi, K. M.; Kim, B. Step-growth polymerization. *Polym. React. Eng.* **2007**, 273−314.
(31) Wagner, H. L. The Mark−Houwink−Sakurada equation for the viscosity of linear polyethylene. *J. Phys. Chem. Ref. Data* **1985**, 14 (2), 611−617.
(32) Tang, D.; Chen, Z.; Correa-Netto, F.; Macosko, C. W.; Hillmyer, M. A.; Zhang, G. Poly(urea ester): A family of biodegradable polymers with high melting temperatures. *J. Polym. Sci. A. Polym. Chem.* **2016**, 54 (24), 3795−3799.

(33) Wandel, M. B.; Bell, C. A.; Yu, J.; Arno, M. C.; Dreger, N. Z.; Hsu, Y.-H.; Pitto-Barry, A.; Worch, J. C.; Dove, A. P.; Becker, M. L. Concomitant control of mechanical properties and degradation in resorbable elastomer-like materials using stereochemistry and stoichiometry for soft tissue engineering. *Nat. Commun.* 2021, 12 (1), 446.

(34) Hsu, Y.-H.; Dove, A. P.; Becker, M. L. Crosslinked internal alkyne-based stereo elastomers: Polymers with tunable mechanical properties. *Macromolecules* 2021, 54 (10), 4649−4657.

(35) Worch, J. C.; Weems, A. C.; Yu, J.; Arno, M. C.; Wilks, T. R.; Huckstepp, R. T. R.; O'Reilly, R. K.; Becker, M. L.; Dove, A. P. Elastomeric polyamide biomaterials with stereochemically tuneable mechanical properties and shape memory. *Nat. Commun.* 2020, 11 (1), 3250.

(36) Bell, C. A.; Yu, J.; Barker, I. A.; Truong, V. X.; Cao, Z.; Dobrinyin, A. V.; Becker, M. L.; Dove, A. P. Independent control of elastomer properties through stereocontrolled synthesis. *Angew. Chem., Int. Ed.* 2016, 55 (42), 13076−13080.

(37) Khalfa, A. L.; Becker, M. L.; Dove, A. P. Stereochemistry-controlled mechanical properties and degradation in 3D printable photosets. *J. Am. Chem. Soc.* 2021, 143 (42), 17510−17516.

(38) *Rubberlike Elasticity: A Molecular Primer*; Wiley: New York, 1988.

(39) Lau, C. M.; Kim, S.-S.; Lillie, L. M.; Tolman, W. B.; Reineke, T. M.; Ellison, C. J. Structural basis for the different mechanical behaviors of two chemically analogous, carbohydrate-derived thermosets. *ACS Macro Lett.* 2021, 10 (5), 609−615.

(40) Utracki, L. A. Introduction to polymer blends. In *Polymer Blends Handbook*; Utracki, L. A., Ed.; Springer Netherlands: Dordrecht, 2003; pp 1−122.

(41) Qiu, Z. In *Crystallization in Multiphase Polymer Systems*; Thomas, S.; Arif P, M.; Gowd, E. B.; Kalarikkal, N., Eds.; Elsevier, 2018; Chapter 8, pp 213−237.

(42) Yao, K.; Nie, H.; Liang, Y.; Qiu, D.; He, A. Polymorphic crystallization behaviors in *cis*-1,4-polyisoprene/*trans*-1,4-polyisoprene blends. *Polymer* 2015, 80, 259−264.

(43) Schyns, Z. O. G.; Shaver, M. P. Mechanical recycling of packaging plastics: A review. *Macromol. Rapid Commun.* 2021, 42 (3), 2000415.

(44) Karaagac, E.; Koch, T.; Archodoulaki, V.-M. The effect of PP contamination in recycled high-density polyethylene (rPE-HD) from post-consumer bottle waste and their compatibilization with olefin block copolymer (OBC). *Waste Manage.* 2021, 119, 285−294.

(45) Xu, J.; Eagan, J. M.; Kim, S.-S.; Pan, S.; Lee, B.; Klimovica, K.; Jin, K.; Lin, T.-W.; Howard, M. J.; Ellison, C. J.; LaPointe, A. M.; Coates, G. W.; Bates, F. S. Compatibilization of isotactic polypropylene (*i*PP) and high-density polyethylene (HDPE) with *i*PP−PE multiblock copolymers. *Macromolecules* 2018, 51 (21), 8585−8596.

(46) Eagan, J. M.; Xu, J.; Di Girolamo, R.; Thurber, C. M.; Macosko, C. W.; LaPointe, A. M.; Bates, F. S.; Coates, G. W. Combining polyethylene and polypropylene: Enhanced performance with PE/*i*PP multiblock polymers. *Science* 2017, 355 (6327), 814.

(47) Kallel, T.; Massardier-Nageotte, V.; Jaziri, M.; Gérard, J.-F.; Elleuch, B. Compatibilization of PE/PS and PE/PP blends. I. Effect of processing conditions and formulation. *J. Appl. Polym. Sci.* 2003, 90 (9), 2475−2484.

(48) Macosko, C. W.; Guégan, P.; Khandpur, A. K.; Nakayama, A.; Marechal, P.; Inoue, T. Compatibilizers for melt blending: Premade block copolymers. *Macromolecules* 1996, 29 (17), 5590−5598.

(49) Xanthos, M.; Dagli, S. S. Compatibilization of polymer blends by reactive processing. *Polym. Eng. Sci.* 1991, 31 (13), 929−935.

(50) Chamas, A.; Moon, H.; Zheng, J.; Qiu, Y.; Tabassum, T.; Jang, J. H.; Abu-Omar, M.; Scott, S. L.; Suh, S. Degradation rates of plastics in the environment. *ACS Sustainable Chem. Eng.* 2020, 8 (9), 3494−3511.

(51) Häußler, M.; Eck, M.; Rothauer, D.; Mecking, S. Closed-loop recycling of polyethylene-like materials. *Nature* 2021, 590 (7846), 423−427.

(52) Brannigan, R. P.; Dove, A. P. Synthesis, properties and biomedical applications of hydrolytically degradable materials based on aliphatic polyesters and polycarbonates. *Biomater. Sci.* 2017, 5 (1), 9−21.

(53) Kosloski-Oh, S. C.; Wood, Z. A.; Manjarrez, Y.; de los Rios, J. P.; Fieser, M. E. Catalytic methods for chemical recycling or upcycling of commercial polymers. *Mater. Horiz.* 2021, 8 (4), 1084−1129.

(54) Worch, J. C.; Dove, A. P. 100th Anniversary of macromolecular science viewpoint: Toward catalytic chemical recycling of waste (and future) plastics. *ACS Macro Lett.* 2020, 9 (11), 1494−1506.

(55) Nowalk, J. A.; Swisher, J. H.; Meyer, T. Y. Influence of short-range scrambling of monomer order on the hydrolysis behaviors of sequenced degradable polyesters. *Macromolecules* 2019, 52 (12), 4694−4702.

(56) Swisher, J. H.; Nowalk, J. A.; Meyer, T. Y. Property impact of common linker segments in sequence-controlled polyesters. *Polym. Chem.* 2019, 10 (2), 244−252.

(57) Washington, M. A.; Swiner, D. J.; Bell, K. R.; Fedorchak, M. V.; Little, S. R.; Meyer, T. Y. The impact of monomer sequence and stereochemistry on the swelling and erosion of biodegradable poly(lactic-co-glycolic acid) matrices. *Biomaterials* 2017, 117, 66−76.

(58) Li, J.; Rothstein, S. N.; Little, S. R.; Edenborn, H. M.; Meyer, T. Y. The effect of monomer order on the hydrolysis of biodegradable poly(lactic-co-glycolic acid) repeating sequence copolymers. *J. Am. Chem. Soc.* 2012, 134 (39), 16352−16359.

(59) Min, K.; Cuiffi, J. D.; Mathers, R. T. Ranking environmental degradation trends of plastic marine debris based on physical properties and molecular structure. *Nat. Commun.* 2020, 11 (1), 727.

(60) Foster, J. C.; Akar, I.; Grocott, M. C.; Pearce, A. K.; Mathers, R. T.; O'Reilly, R. K. 100th Anniversary of macromolecular science viewpoint: The role of hydrophobicity in polymer phenomena. *ACS Macro Lett.* 2020, 9 (11), 1700−1707.

(61) Yildirim, E.; Dakshinamoorthy, D.; Peretic, M. J.; Pasquinelli, M. A.; Mathers, R. T. Synthetic design of polyester electrolytes guided by hydrophobicity calculations. *Macromolecules* 2016, 49 (20), 7868−7876.

(62) Magenau, A. J. D.; Richards, J. A.; Pasquinelli, M. A.; Savin, D. A.; Mathers, R. T. Systematic insights from medicinal chemistry to discern the nature of polymer hydrophobicity. *Macromolecules* 2015, 48 (19), 7230−7236.